
Research article

Maximum shear modulus (G_0) determination by different in situ testing techniques in two tropical soil sites

Breno Padovezi Rocha^{1,*}, Luis Pedro Rojas Herrera² and Heraldo Luiz Giacheti²

¹ São Paulo State University (UNESP), School of Engineering, Department of Civil Engineering, Ilha Solteira, SP, Brazil

² São Paulo State University (UNESP), School of Engineering, Department of Civil and Environmental Engineering, Bauru, SP, Brazil

* Correspondence: Email: breno.rocha@unesp.br; Tel: +5517991176996.

Abstract: Geotechnical site characterization requires the determination of the stratigraphic profile, the groundwater level position, and the appropriate geomechanical design parameters required for each project. It is also necessary to assess both the spatial and temporal site variability. The shear wave velocity profile (V_s) and, consequently, the maximum shear modulus (G_0) are very important parameters for geotechnical projects. Although a large part of Brazil is covered by tropical soils, the literature on the dynamic behavior of these soils is limited. The seismic dilatometer test (SDMT) has been used in several site investigation campaigns, both at research test sites and in construction projects. This paper presents comparisons of the maximum shear modulus (G_0) profiles at two well-documented tropical soil sites using the SDMT and other in situ testing techniques such as the crosshole (CH) and downhole (DH) methods, the seismic piezocone penetration test (SCPTu), and seismic standard penetration tests (SSPTs). G_0 measurements obtained with the SDMT were found to be generally accurate and in good agreement with the CH, DH, SCPTu, and SSPT data used as references in the comparisons. Furthermore, this paper shows that the classical empirical correlations used to estimate G_0 from the intermediate parameters (E_D , K_D , and M_{DMT}) of the flat dilatometer test (DMT) were not able to estimate G_0 for both studied sites. This may be related to the presence of microstructure (e.g., cementation/bonding and aging) as well as a possible soil suction influence typical of the investigated tropical soil sites. The G_0/E_D and G_0/M_{DMT} ratios determined by the SDMT were used to assess the presence of microstructure and any possible soil suction influence. In addition, an equation was proposed to estimate G_0 from the intermediate DMT parameters.

Keywords: site investigation; maximum shear modulus; crosshole; downhole; seismic standard penetration tests; SDMT

1. Introduction

Elastic soil parameters, such as the maximum shear modulus (G_0) and the modulus degradation curve (G/G_0 vs. γ), are extremely important in evaluating the mechanical behavior of soils under dynamic loads, such as earthquake engineering problems, static deformation, slope stability, non-textbook behavior, as well as in identifying collapsible soils [1–4]. In Brazil, the growing demand for geotechnical projects focusing on soil dynamics makes it necessary to learn more about the different testing techniques and how to interpret their results. Knowledge of stiffness degradation is critical in the design of geotechnical projects [5,6]. G_0 is the stiffness parameter that refers to the initial undisturbed state of the soil and allows the assessment of the stress–strain–resistance behavior of the soil for static, cyclic, and dynamic loading under both drained and undrained conditions [7].

There are several in situ techniques available for evaluating the G_0 profile, such as the crosshole (CH) and downhole (DH) methods, the seismic standard penetration test (SSPT), spectral analysis of surface waves (SASW), the seismic cone penetration test (SCPT), and the seismic dilatometer test (SDMT) [8–10]. Each technique has its own advantages and limitations, and the results may not be consistent in many cases due to scale problems and differences among the tests, so it is important to select an appropriate in situ testing technique that considers the site conditions and the importance of the projects to obtain a reliable G_0 profile [4].

Most of the Brazilian territory is covered by tropical soils, which are geomaterials with unusual behavior compared with soils formed in temperate zones. Temperature variations and intense chemical decomposition of rocks result in deeper layers of weathered materials, which include lateritic and saprolitic soils. The lateritic soils can be either residual or transported and are characterized by the laterization process, which is an enrichment of a soil with iron and aluminum and their associated oxides, caused by weathering in regions that are hot, acidic, and at least seasonally humid [11]. In addition, lateritic soils can have a porous macrostructure that can collapse upon saturation. However, saprolitic soils are residual and retain a relic structure of the parent rock. Tropical soils present a peculiar behavior due to the geological and/or pedological processes inherent to their formation and to their unsaturated condition, which means that classical soil mechanics has limitations in predicting such behavior [11,12].

This paper presents the crosshole (CH) and downhole (DH) tests, SCPT, SSPT, and SDMT carried out in two tropical Brazilian soil sites. The advantages and limitations of the test procedures and their interpretation are briefly discussed, and the differences observed among the G_0 profiles obtained by these techniques are also discussed. The paper also discusses the use of the G_0/E_D and G_0/M_{DMT} ratios as useful indices for site characterization of tropical soils, and presents and discusses adaptations to the classical empirical correlations for estimating G_0 from the DMT's intermediate parameters.

2. Seismic in situ testing techniques

The shear wave velocity (V_s) and, consequently, the maximum shear modulus (G_0) have been used in several geotechnical works (seismic site assessment, pile driving, collapsible soil identification, and state

parameter identification). The maximum shear modulus can be calculated from V_s using Eq. 1:

$$G_0 = \rho \cdot V_s^2 \quad (1)$$

where V_s is the shear wave velocity (m/s), and ρ is the soil density (kg/m^3), which can be determined from undisturbed soil samples collected in sample pits.

2.1. Crosshole seismic tests

The CH seismic test, also known as seismic test between boreholes, is one of the most effective methods for in situ G_0 determination. The main purpose of this technique is to determine the compression (P -) and/or shear (S -) waves' velocities at depth, and was standardized by [13].

The test consists of generating seismic waves in boreholes and measuring the time a wave takes to propagate from one borehole to two seismic transducers located in two other boreholes that are at the same depth as the seismic source. The distance between the source borehole and the first transducer (receiver borehole) should be between 1.5 and 3 m, and the distance between the subsequent transducers should be between 3 and 6 m [13]. The source and the seismic transducers (geophones) are positioned at the same elevation, and the determination of V_s is performed every meter. In addition, a two-borehole configuration (one for the seismic source and another for the receiver) can also be used [13].

Special care should be taken when drilling and preparing these boreholes. The procedure suggested by ASTM 4428 [13] is to cover them with metal or polyvinyl chloride (PVC) pipes, fixed to the ground with cement grout (Figure 1).

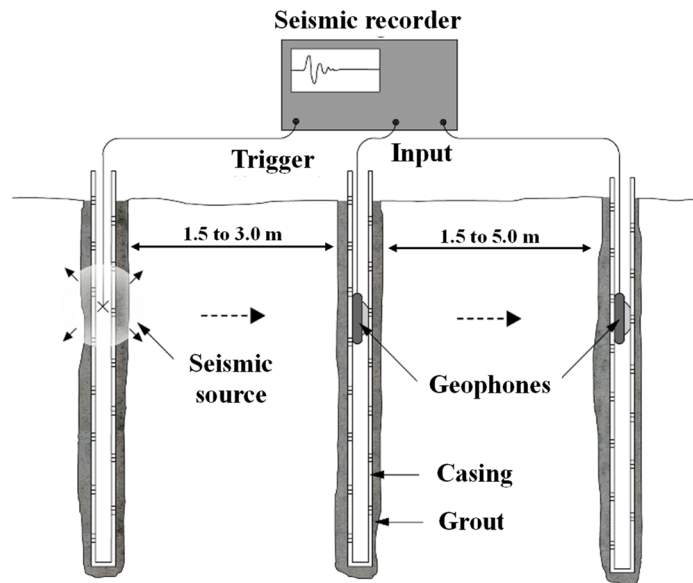


Figure 1. Schematic representation of the crosshole test (adapted from [13]).

2.2. Downhole seismic test

The DH seismic test is performed in a single borehole instead of three [14]. It is similar in several respects to the CH seismic test method [12]. The test consists of determining the arrival of the seismic wave train generated at the surface and received by one or more seismic transducers positioned at

different depths. When interpreting the results, it is assumed that the path traveled between the source and the receiver is in a linear trajectory.

The determination of shear wave velocities can be carried out using three different methods: First arrival time, crossover, and cross-correlation. The cross-correlation method outperforms the others, as it is less affected by distortions in the signal, leading to more consistent and reliable results [15].

2.3. Seismic piezocone penetration test

The piezocone penetration test (CPTu) is a standard instrumented probe with a 60° apex and a typical diameter of 35.7 mm (10 cm² area) at the end of a series of rods. The probe is pushed into the soil at a constant rate of 20 mm/s by a hydraulic pushing source. Tip resistance (q_c), sleeve friction (f_s), and pore water pressure (u) are continuously monitored and typically digitized at 20-mm intervals. In the mid-1980s, a seismic wave acquisition system was incorporated into the electric cone or piezocone, which became known as the seismic piezocone test (SCPTu). The shear wave velocity, and hence the maximum shear modulus of the soil, can be determined quickly, accurately, and with a high level of repeatability [15]. The seismic piezocone has the same characteristics as a standard piezocone but differs from it by the insertion of a geophone or accelerometer inside.

The use of the downhole technique during the SCPTu basically involves three steps standard penetration tests measuring the arrival time of the S -waves, determining the S -wave velocity (V_s) at each test depth, and calculating the maximum shear modulus (G_0) for each of these depths. Each of these steps has uncertainties and can lead to cumulative errors that must be reduced. A diagram of how the downhole test is performed during the SCPT is shown in Figure 2.

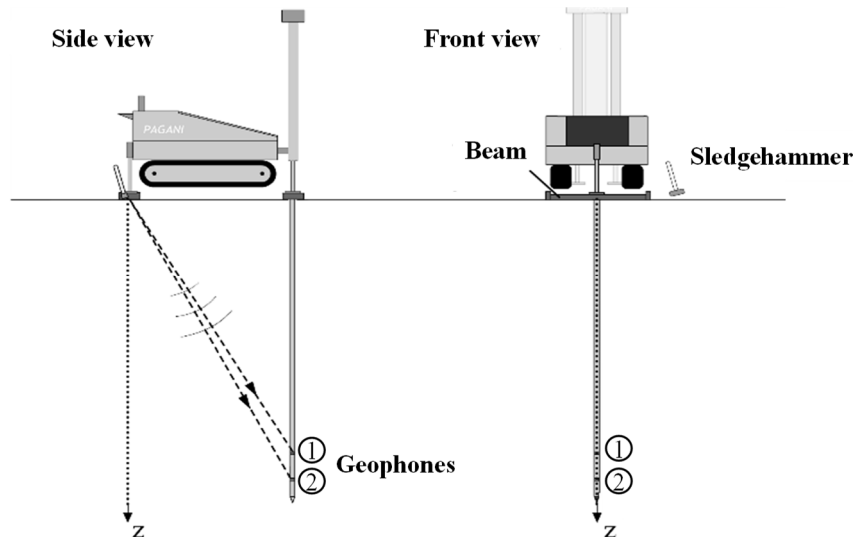


Figure 2. Schematic representation of the downhole test (adapted from [16]).

2.4. Seismic standard penetration test

The standard penetration test (SPT) with an uphole seismic technique (SSPT) is an old but little-used resource. The technique is described in detail in [4,17]. The test is performed at each depth of the SPT (typically every meter), where a seismic wave is generated, which is captured and acquired at the

surface using seismic transducers (geophones) and a data acquisition system. A schematic representation of the SSPT test is shown in Figure 3.

The equipment used to perform the SSPT test is the same as that used to perform the conventional SPT. The seismic waves are generated by the impact of a 2-kg sledgehammer on the SPT anvil. The determination of the V_s profile requires the determination of the propagation path of the wave through the soil mass, as the seismic transducers are located far from the borehole, as well as the arrival time of the shear waves. Bang and Kim [4] described two methods for this calculation: DTR (delay time between serial receivers) and DTS (delay time between serial sources). Pedrini et al. [17] suggested using the DTS method, in which the exact moment of arrival of the shear wave is determined by plotting the seismic signals captured at different depths.

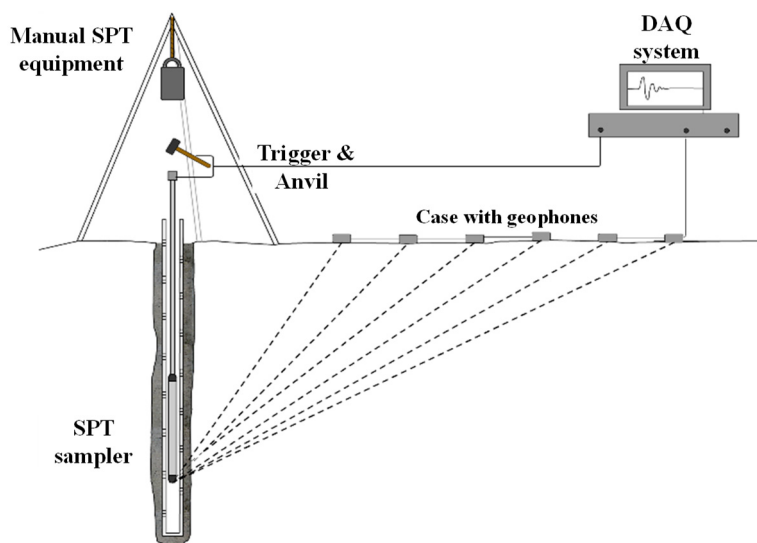


Figure 3. Schematic representation of the downhole test (adapted from [17]).

Figure 4 shows a typical profile of these signals, captured by a geophone positioned 10.5 m away from the borehole, as well as the arrival point of the shear wave. More details on the interpretation and execution of SSPTs can be found in Bang and Kim [4] and Pedrini et al. [17].

Typical wave profile and the identification of the minimum point of the S waves – Geophone positioned 10.5 m from the borehole

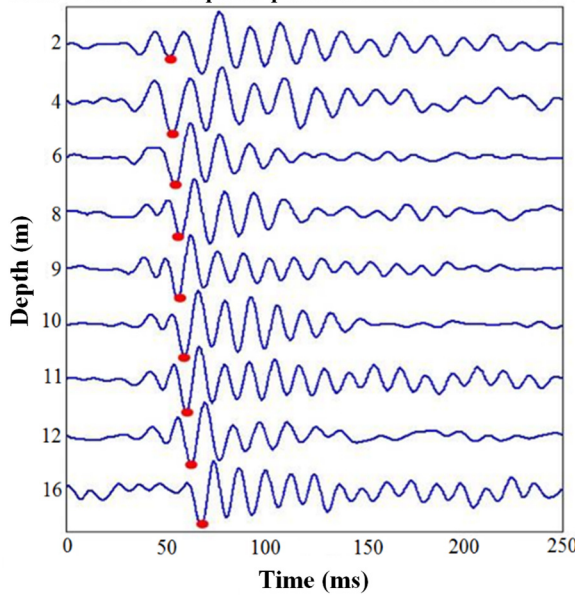


Figure 4. Schematic representation of the downhole test (adapted from [17]).

2.5. Flat dilatometer and seismic dilatometer

The flat dilatometer test (DMT) consists of driving the dilatometer's blade using a hydraulic system and a push rig. The dilatometer is advanced into the soil using common field equipment. The penetration rate is usually 2 cm/s (rates from 1 to 3 cm/s are acceptable [18]), and at every 20 cm, the drive is interrupted and gas pressure is applied through a control unit, inflating the membrane through a hose that goes inside the rod used to drive the blade into the ground. The pressures required for the membrane to lose contact with the sensitive equipment (p_0) and the pressure required for the membrane to move 1.1 mm (p_1) are determined [18]. From these readings, the intermediate parameters (I_D , K_D , and E_D) are calculated, which are used to classify the soil and estimate the geotechnical parameters [18].

$$I_D = \frac{p_1 - p_0}{p_0 - u_0} \quad (2)$$

$$K_D = \frac{p_0 - u_0}{\sigma' v_0} \quad (3)$$

$$E_D = 34.7 (p_1 - p_0) \quad (4)$$

where u_0 is the in situ pore water pressure, and $\sigma' v_0$ is the effective vertical stress.

The SDMT uses the combination of the standard DMT equipment with a seismic module to measure the shear wave velocity (V_s) (Figure 5) [19]. The seismic module is a cylindrical element placed above the DMT blade and equipped with two receivers at 0.5-m intervals.

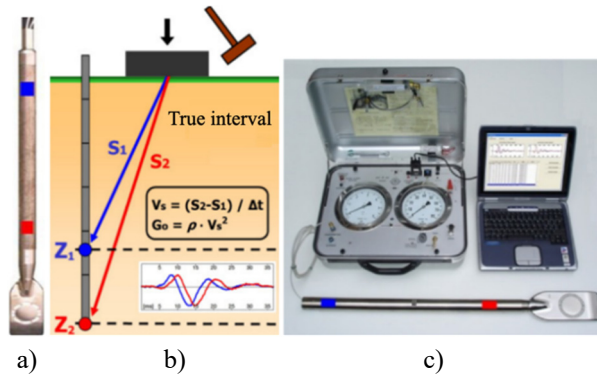


Figure 5. (a) Dilatometer blade with seismic module; (b) schematic representation of the SDMT's execution; (c) seismic dilatometer equipment (adapted from [10]).

2.5.1. Estimating G_0 by DMT

The maximum shear modulus can be estimated by the flat dilatometer or the seismic dilatometer on the basis of correlations presented by Monaco et al. [20]. Equations 5, 6, and 7 can be used to estimate G_0 from the ratio G_0/M_{DMT} vs. K_D for clay, sand, and silt soils, respectively. The G_0/M_{DMT} ratio depends on both the soil type and stress history [18] (Figure 6).

Most empirical correlations used to estimate V_s and G_0 are developed from soils with little or no microstructure, according to Robertson [21]. Several studies have demonstrated the influence of the structure on the mechanical behavior of soils under natural or compacted conditions [22–25]. The term “structure” is used to define the combination of the words “fabric” (the arrangement of particles) and “bonding” (the interparticle forces that are not frictional in nature) [26]. Structure is directly related to the soil formation process (sedimentary, residual, and/or pedogenetic evolution). These correlations should be used with caution, as G_0 may be underestimated in highly structured soils. The measured V_s (and therefore G_0) is highly sensitive to the presence of microstructure (e.g., cementation/bonding and aging) in the soil [21,27].

Berisavljević and Berisavljević [27] show that the boundary separating soils with and without a significant presence of microstructure can be drawn at a $G_0\text{measured}/G_0\text{estimated}$ ratio of 1.5; however, according to the authors' experience, a $G_0\text{measured}/G_0\text{estimated}$ higher than 1.3 could be the boundary separating soils with and without the significant presence of microstructure. Thus, the comparison between the maximum shear modulus obtained from V_s using Eq. 4 and estimated by the DMT (Figure 6) can be directly used to detect soils that behave differently from “ideal” soils, i.e., soils without a significant presence of microstructure.

$$\frac{G_0}{M_{DMT}} = 26.177 K_D^{-1.0066} \quad (5)$$

$$\frac{G_0}{M_{DMT}} = 4.5613 K_D^{-0.7967} \quad (6)$$

$$\frac{G_0}{M_{DMT}} = 15.686 K_D^{-0.921} \quad (7)$$

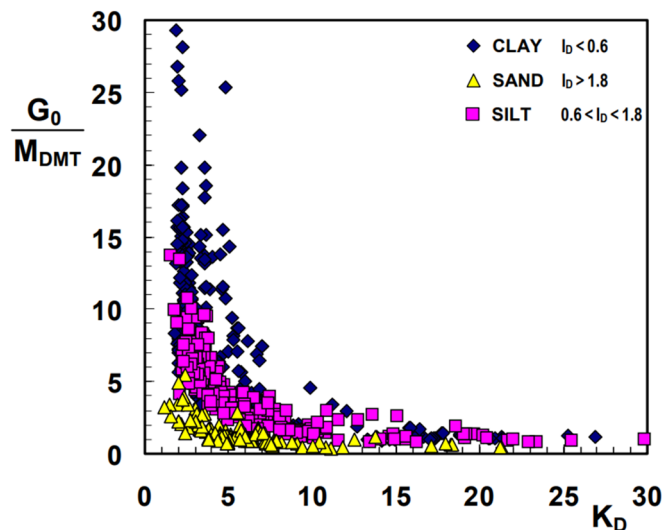


Figure 6. G_0/M_{DMT} vs. K_D for clay, silt, and sandy soils (adapted from Monaco et al. [20]).

3. Description of sites and tests

3.1. Sites

Two research sites located on two university campuses in the State of São Paulo, Brazil, were studied: the Universidade Estadual Paulista (UNESP) Bauru research site and the Universidade de São Paulo (USP) São Carlos research site.

The soil profile at the UNESP research site consists of an unsaturated red clayey fine sand. The upper 13 m is a colluvial soil (Cenozoic sediment) with lateritic behavior overlying a residual soil from Sandstone with nonlateritic behavior [28]. This soil is classified as SM-SC (silty sands to clayey sands) according to the Unified Soil Classification System. Another important aspect at this site is the horizontal variability of the soil's behavior, which is evident when analyzing, for example, q_c records in tests with the electric piezocone penetration test (CPT), as discussed by De Mio [29]. The water table at this site is deeper than 20 m.

The subsoil profile of the USP research site consists of clayey fine sand with two well-defined layers, namely Cenozoic sediments (colluvium) with a lateritic behavior overlying the residual soil derived from sandstone (non-lateritic behavior) [29]. A 0.2–0.5-m thick layer of pebbles separates the surface layer from the residual soil. The water table varies seasonally between 9 and 12 m below the ground surface. Both layers are classified as clayey sand (SC) according to the Unified Soil Classification System. The interpretation of the MCT (Miniature, Compacted, Tropical) classification test [30] data separated the lateritic (LA') from the non-lateritic (NA') soil behavior approximately at a depth of 6 m.

It is important to note that both subsoils are mostly partially saturated, so it was assumed that the measured cone tip resistance (q_c) was equal to the corrected cone tip resistance (q_t), since pore pressure was not measured. The friction ratio (R_f) was calculated as $f_s/q_t \times 100\%$.

Figures 7 and 8 show the results of the SPTs, CPTs, and flat dilatometer tests (DMTs) previously performed at the UNESP and USP research sites, respectively. Cone tip resistance (q_c) and the sleeve

friction (f_s) tend to increase with depth. The friction ratio ($R_f = f_s/q_t \times 100\%$) varies between 4 and 8%. N -values from the SPTs and p_0 and p_1 from the DMTs increase almost linearly with depth.

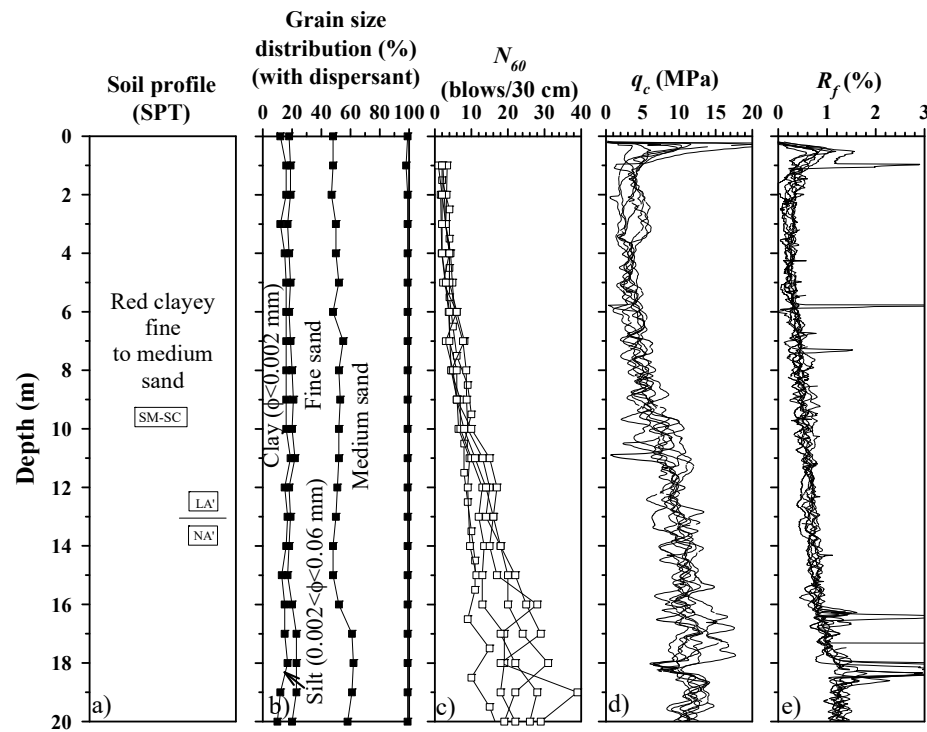


Figure 7. Summary of tests performed at the UNESP research site (adapted from [17,31]).

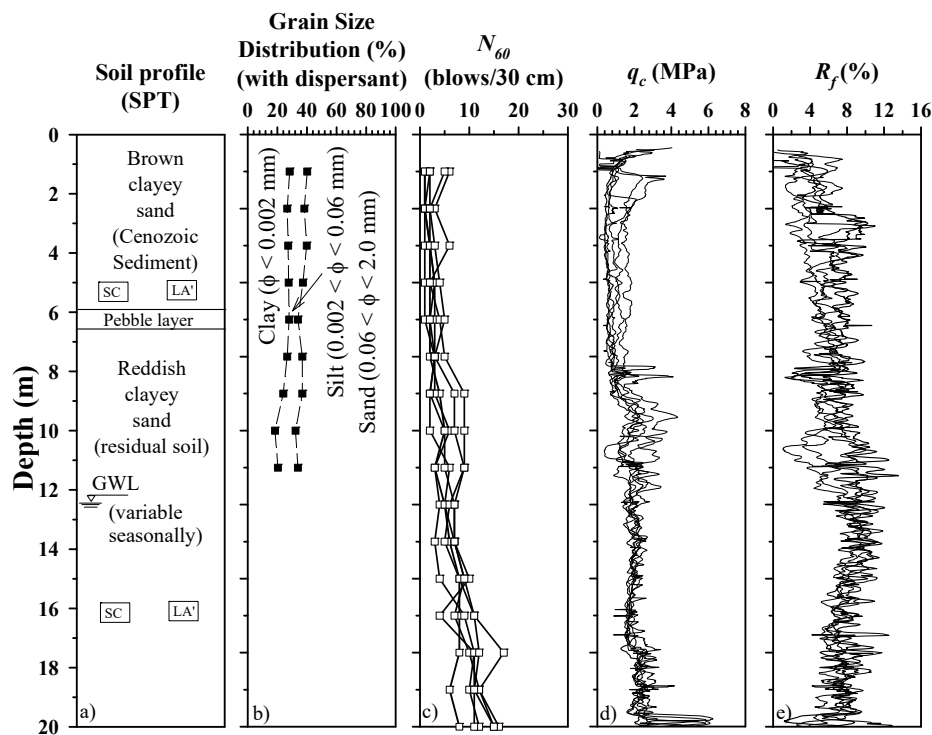


Figure 8. Summary of tests performed at the USP research site (adapted from [17,32]).

3.2. *In situ* seismic tests

Several seismic tests were conducted at both research sites. At the UNESP research site, nine seismic tests were conducted: one CH test (CH 1), two DH test (DH 1 and DH 2), one SCPT (SCPT 1), one SSPT (SSPT 1), and four SDMTs (SDMT 1, SDMT 2, SDMT 3, and SDMT 4). The crosshole test was conducted to a depth of 14 m, while the other tests were conducted to a depth of 20 m. Ten seismic tests were conducted at the USP research site: two crossholes (CH 1 and CH 2), two downholes (DH 1 and DH 2), one seismic cone (SCPT 1), one SSPT (SSPT 1) and four seismic dilatometers (SDMT 1, SDMT 2, SDMT 3 and SDMT 4). The two CH tests were conducted to a depth of 9 m, while the other tests were conducted to a depth of 20 m.

The CH seismic tests were performed according to the recommendations given by [11] (i.e., three boreholes spaced 3 m apart, using a grout mix that closely matches the formation density). At both sites, the boreholes were drilled with a 150-mm diameter, the two receiver boreholes were cased with PVC pipe 75 mm in diameter, and the source borehole was cased with PVC pipe 85 mm in diameter.

The downhole tests were performed using a seismic probe with three geophone compartments, spaced 0.5 m apart [33]. This probe allows three recordings for each test depth. The seismic source was a steel rod (shear beam) placed on the ground surface 0.3 m away from the borehole opening. The data were interpreted using the cross-correlation and the true interval methods. The DH tests were conducted to a depth of 18 m. For more information on the DH test equipment and procedures, see Vitali et al. [33].

A 100 kN CPTu seismic probe with a 10-cm² cross-section area was used to measure the tip resistance (q_c) and sleeve friction (f_s). Pore pressure (u) was not recorded because the water table was deeper than 10 m depth at all sites. A self-anchoring multi-purpose push platform with a 200-kN hydraulic system capacity was used to push the probe. The seismic receivers within the cone consisted of a triaxial geophone. A mechanical swing hammer with a single hammer weight and drop height was used as the seismic wave source. The arrival time of the shear waves was also determined using the reversible impulse criterion. To eliminate unwanted noise and maintain a quality signal, the hammering was repeated at each depth. After removing the noise data, two repeatable seismic signals obtained from two blows for each side of the plate at a given depth were interpreted using the crossover technique [15]. The SCPTs were conducted to a depth of 16 m.

An SSPT is a hybrid test that incorporates the uphole seismic technique for determining V_s values during the traditional SPT. However, a seismic wave is generated at each depth (typically at every meter), and it can be recorded on the ground surface. The equipment used to perform this test is the same as the one currently used for the conventional SPTs, including an array of transducers (usually geophones) placed in appropriate boxes on the ground surface, a trigger system (digital or analog), and the seismic source, which is the SPT sampler itself. The SSPT tests have been conducted to depths of up to 20 m. For more information on the SSPT's test equipment and procedures, see Bang and Kim [4] and Pedrini et al. [17].

SDMTs were performed to a 20-m depth. The seismic source was the same as that used in the DH test. It was oriented with its long axis parallel to the axis of the receivers to provide the highest sensitivity to the generated shear wave. The time delay of the SDMT seismograms was determined using the cross-correlation algorithm.

4. Results and discussion

4.1. Shear wave velocity and maximum shear modulus profiles

The results of the seismic test campaigns carried out at the UNESP research site (Figure 9a,b) and the USP research site (Figure 10a,b) are graphically presented, showing the values of V_s and, consequently, G_0 , along the depth. The profiles of G_0 (Figure 9b and Figure 10b) were calculated from the V_s values, and the natural specific mass values of the soil were determined from undisturbed samples collected from exploratory sample pits [34]. The G_0 measurements obtained via the SDMT were found to be generally accurate and in close agreement with the CH, DH, SCPT, and SSPT results, which were used as references in the comparisons. The differences in V_s and G_0 can be attributed to the different directions of propagation and polarization of the shear waves induced by CH and DH tests and the SSPT, SCPT, and SDMT. In addition, these differences can also be explained by the unsaturated condition and inherent variability [35,36].

There was a progressive increase in the values of V_s and G_0 with depth, followed by a tendency to stabilize after a certain depth. For the USP research site, it is possible to note an upper layer that reaches a depth of 9 m. In the upper layer, V_s ranged from 194 to 305 m/s, with an average velocity of 275 m/s. In the lower layer (between 9 and 18 m in depth), V_s ranged from 270 to 370 m/s, with an average velocity of 325 m/s. For the UNESP research site, there was a progressive increase in the values of V_s and G_0 up to about 12 m, followed by a tendency to stabilize after this depth. In the upper 12 m, V_s ranged from 150 to 420 m/s, with an average velocity of 310 m/s, and V_s ranged from 320 to 382 m/s, with an average velocity of 351 m/s below 12 m in depth.

The maximum shear modulus shows a similar behavior. For the UNESP research site, G_0 ranged from 60 to 250 MPa up to 12 m in depth, with an average of 182 MPa, and 180 to 325 MPa below 12 m in depth. However, for the USP research site, G_0 ranged from 62 to 196 MPa, with an average of 140 MPa up to 9 m, and G_0 ranged from 151 to 224 MPa, with an average velocity of 205 MPa below 9 m in depth.

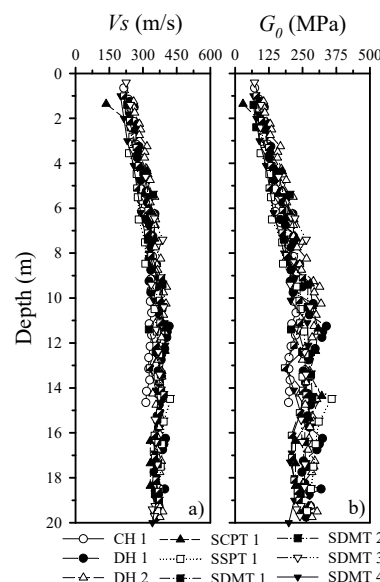


Figure 9. V_s and G_0 measured by CH, DH, SCPT, SSPT, and SDMT for the UNESP research site.

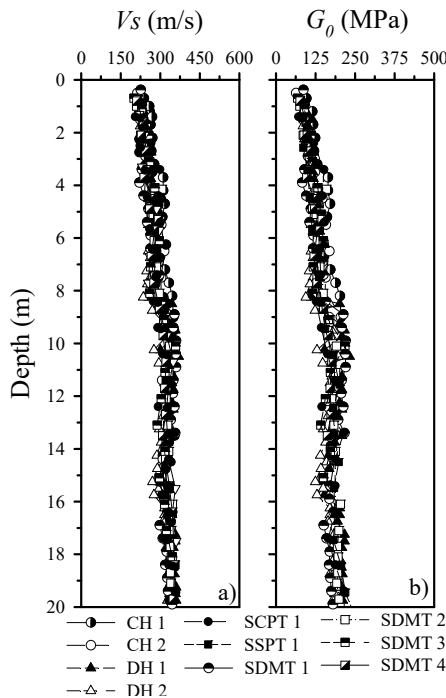


Figure 10. V_s and G_0 measured by CH, DH, SCPT, SSPT, and SDMT for the USP research site.

According to the V_s and G_0 profiles for both sites, the SDMT proved to be an interesting alternative for determining the V_s profile and, consequently, G_0 . The hybrid tests include both geotechnical and geophysical data and provide a convenient and efficient means of obtaining a large amount of geotechnical information with depth from a single sounding: p_0, p_1 , and V_s . They are also less costly than CH tests, since this test requires the preparation of boreholes, as mentioned above.

4.2. Estimates of G_0 from SDMT's intermediate parameters

As discussed in the previous section, the SDMT proved to be an effective method for determining V_s and, consequently, G_0 . However, techniques for measuring V_s are not always available, so it is necessary to use correlations to estimate this parameter. In this regard, the equations proposed by Monaco et al. [20] (Figure 6) were used to determine G_0 (G_{0est}) for both experimental sites studied. It should be noted that for the estimation of G_0 , the soil was considered to be sandy silt (silty soil), due to the classification of the soils of the two experimental sites using the material index (ID).

The measured and estimated G_0 profiles are shown in Figures 11 and 12 for the UNESP and USP research sites, respectively. The four SDMT tests performed in each experimental research site were used in this analysis. As previously presented, for the UNESP research site, the measured G_0 profiles increased almost linearly with depth, up to about 12 m, while for the USP research site, the G_0 profiles increased almost linearly with depth up to about 9 m. The estimated shear modulus profiles, however, tended to increase gradually with depth from the soil surface for both sites.

Despite the soil's variability and uncertainty due to the local site conditions, the G_{0mea}/G_{0est} ratio is higher than 1.3 up to 10 m depth at UNESP and up to 12 m depth at the USP research site. The differences between G_{0mea} and G_{0est} are related to the presence of microstructure (e.g., bonding, cementation, and aging) in the soil. In addition, the effect of the microstructure is more pronounced in

the upper layers and mainly affects the measured G_0 values (G_{0mea}). Confinement governs the mechanical behavior of the soil with increasing depth, affecting the intermediate parameters of DMT (I_D , K_D , and E_D) and, consequently, the estimated values of G_0 (G_{0est}). Therefore, the values of the relationship tend to decrease with depth. The tropical soil sites studied present a peculiar behavior due to the geological and/or pedological processes inherent in their formation, resulting in an open unstable structure and unsaturated conditions. Particles are held in position in the soil structure by bonds that can provide temporary additional strength. Such bonds can be created by soil suction and/or by cementing substances such as iron oxides [11,30]. Thus, the classical correlations suggested for ideal soils (Figure 6) should be used with caution when there is an indication that the soil is structured, such as the tropical soil sites studied.

4.2.1. $G_0/MDMT$ versus K_D and G_0/E_D versus I_D for identification of the microstructure

According to Robertson [21], it is important to identify the level of microstructure in a soil profile, because if soils have little or no microstructure, the classical approaches to interpreting in situ tests, such as the CPT and DMT, can provide reasonable estimates of soil behavior. However, when soils have a significant microstructure, the classical approaches are not always applicable and site- or geology-specific modifications may be required.

The charts developed by [37] were used to verify the distinct behavior of the investigated tropical soil sites. The authors proposed two charts for the detection of microstructure on soils based on DMT and SDMT data as well as a DMT calibration experiment carried out inside an artificially cemented block sample prepared in a large chamber (CemSoil box).

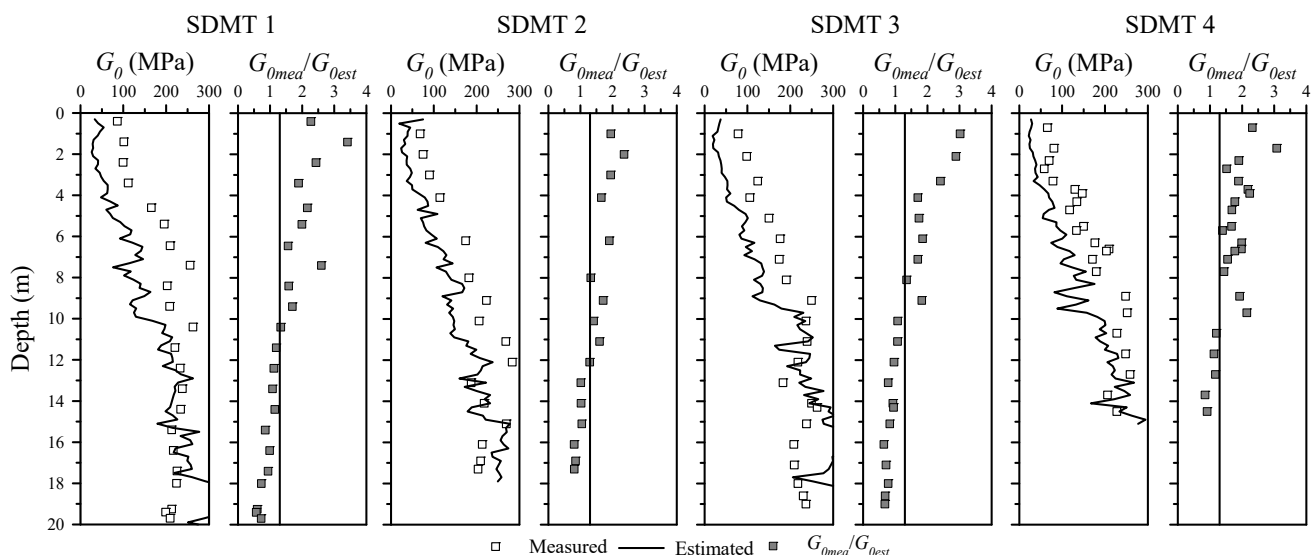


Figure 11. Estimated and measured G_0 as well as G_{0mea}/G_{0est} ratios for the UNESP research site.

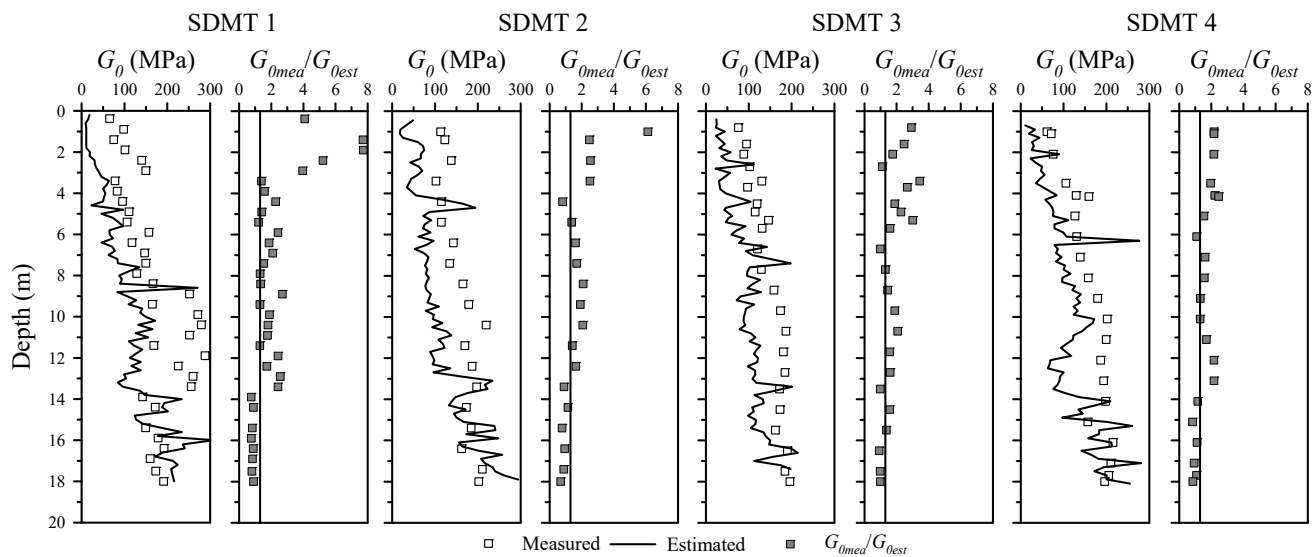


Figure 12. Estimated and measured G_0 as well as $G_{0\text{mea}}/G_{0\text{est}}$ ratios for USP research site.

Figures 13 and 14 show the G_0/E_D vs. I_D (Figures 13a and 14a) and G_0/M_{DMT} vs. K_D (Figures 13b and 14b) charts for the UNESP and USP research sites, respectively. In both charts, the plotted SDMT data from the UNESP and USP sites are above the equation line (the borderline) that separates soils with a microstructure from those without a microstructure, indicating that the bounded structure of the studied tropical sandy soils produces G_0/E_D and G_0/M_{DMT} values that are systematically higher than those measured in soils with little or no microstructure (e.g., the drained and undrained mechanical behavior of sedimentary clays and the drained response of reconstituted sands).

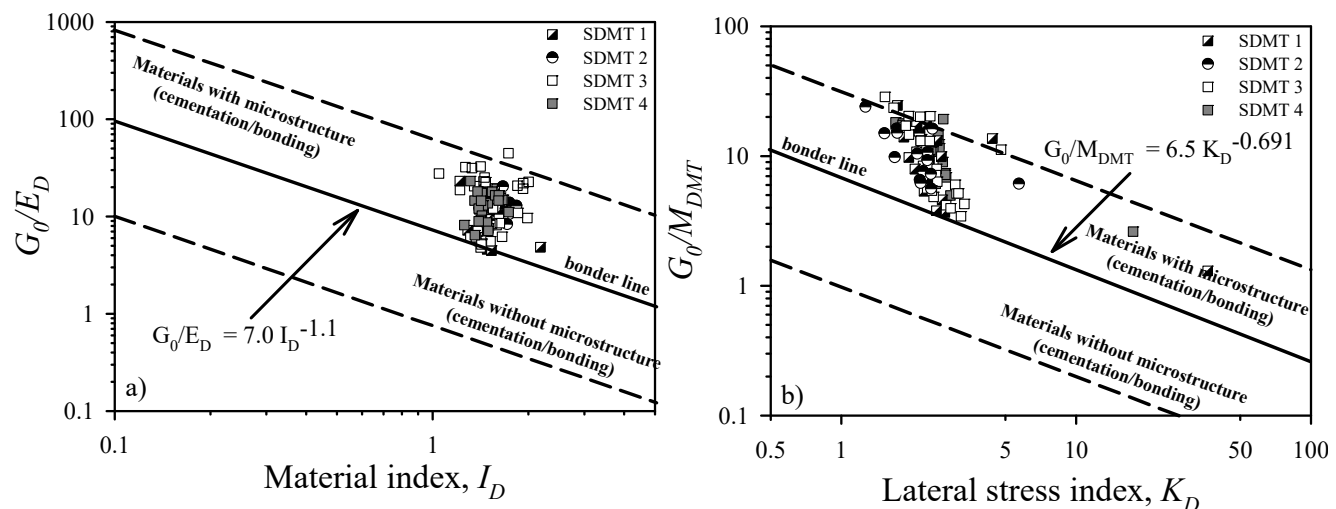


Figure 13. SDMTs performed in the UNESP research site plotted on a G_0/E_D vs. I_D chart (a) and a G_0/M_{DMT} vs. K_D chart (b) (adapted from [37]).

4.3. New correlations to estimate G_0 from DMT

The classical correlations available to estimate G_0 from the DMT (Figure 6) were less reliable, as shown in Figures 10 and 11, and local modification is needed. Following the work of Monaco et al. [20], the values of the G_0/M_{DMT} ratio (164 data points) are plotted in Figure 15 as a function of the horizontal stress index K_D . The best fitting equation (Eq. 5) is given for the soils studied. Similar to the trends presented by Monaco et al. [20], G_0/M_{DMT} decreases with increasing K_D (related to overconsolidation ratio - OCR). In addition, the G_0/M_{DMT} ratio varies across a wide range (≈ 0.6 to 65). As discussed by these authors, it seems almost impossible to estimate G_0 by multiplying the operative modulus (M_{DMT}) by a constant value, as suggested by several authors [38–41].

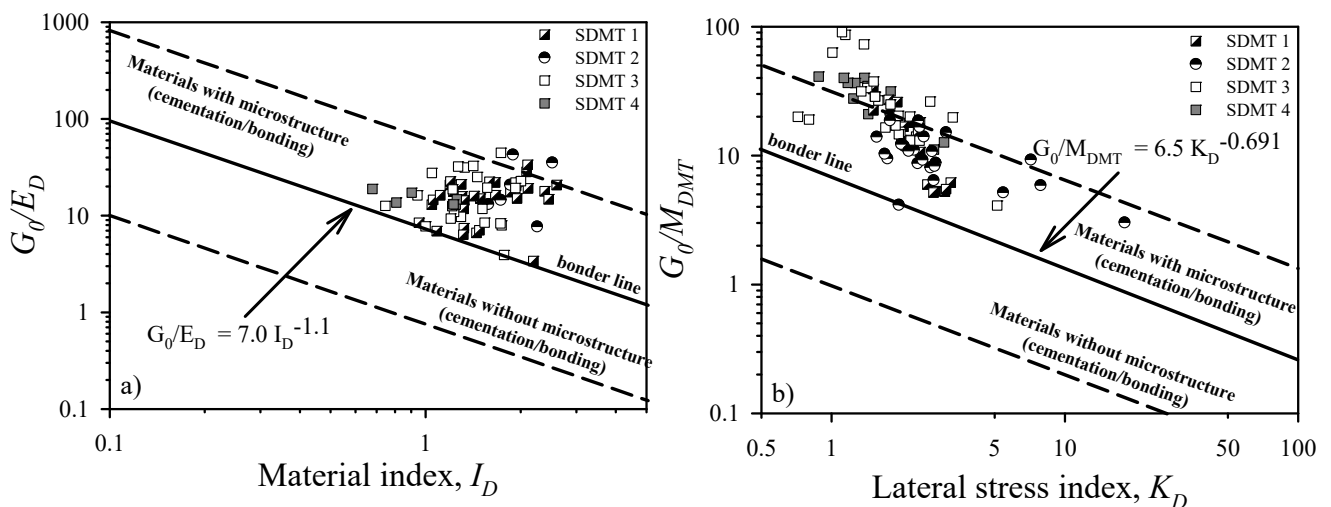


Figure 14. SDMTs performed in the USP research site plotted on a G_0/E_D vs. I_D chart (a) and a G_0/M_{DMT} vs. K_D chart (b) (adapted from [37]).

$$G_0/M_{DMT} = A \cdot K_D^{-B} \quad (5)$$

where A and B are constants which differ depending on the soil type.

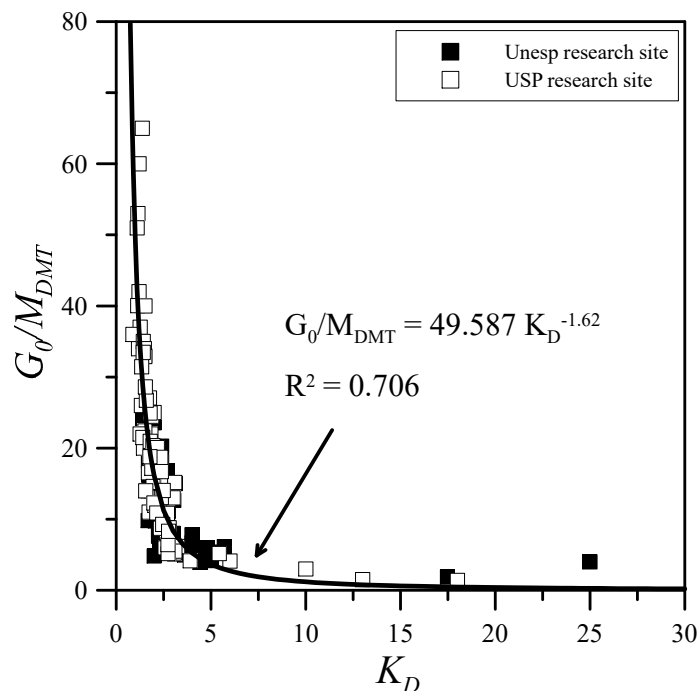


Figure 15. G_0/M_{DMT} ratio vs. K_D for the studied soil sites.

The G_0/M_{DMT} ratios and the constants A and B taken from Marchetti et al. [10], Cruz et al. [37], Berisavljević et al. [42], Mlynarek et al. [43], and this study are shown in Table 1 for the clay, silt, sand, and sandy silt soil types. Cruz et al. [37] used the G_0/M_{DMT} ratio to distinguish residual (cemented) soils from unstructured sedimentary soils, from I_D up to 1.2. Berisavljević et al. [42] studied the collapsible loess from the Zemun loess plateau in Serbia. Mlynarek et al. [43] studied a wide range of soils of different origin in Poland. For the investigated soils (this study), the best fitting equation is represented by Eq. 5, where $A = 49.587$ and $B = -1.62$, as shown in Table 1.

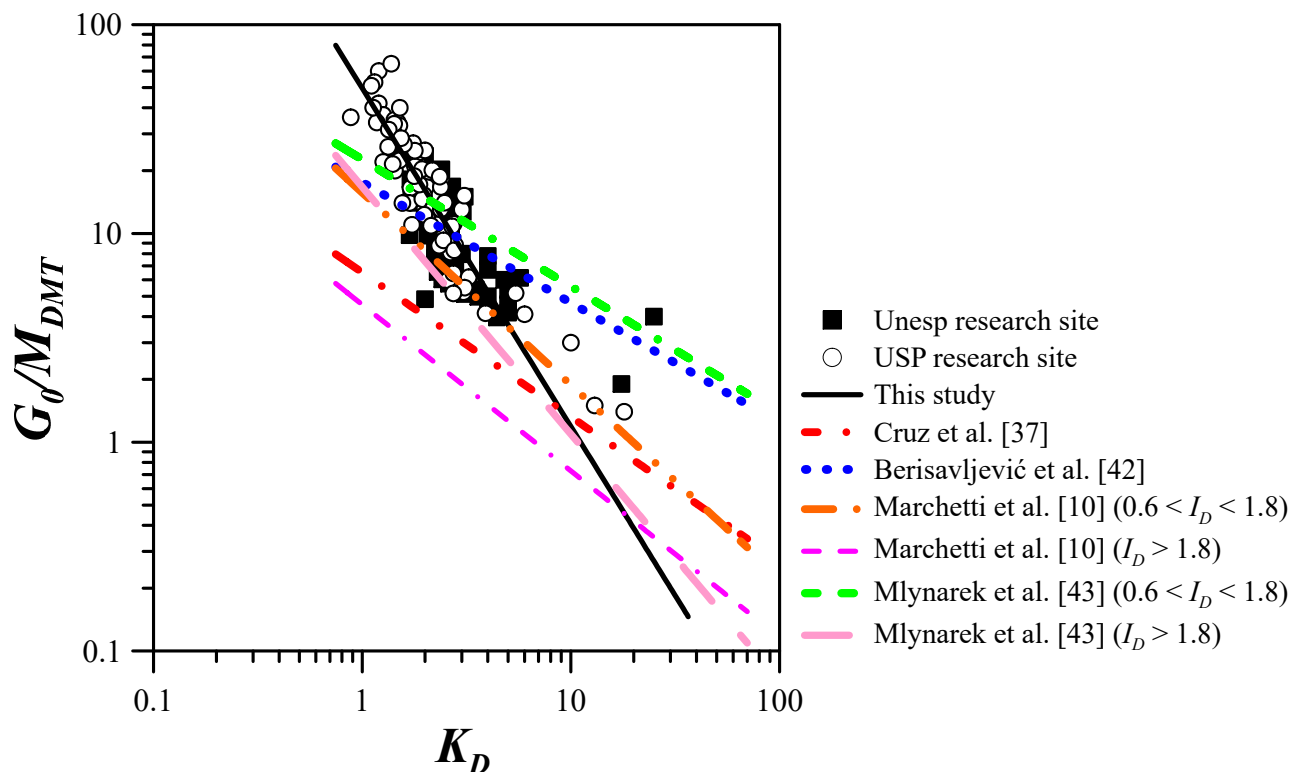
The constants A and B for sandy silts (this study) are very different from the other soils shown in Table 1. These trends may indicate that the soils studied have unusual behavior (cementation/bonding and/or aging). In Table 1, the G_0/M_{DMT} ratios for sandy silts (this study) are much higher than those of sands, both represented by $I_D > 1.8$, and even higher than those of clays, where the widest range in the G_0/M_{DMT} ratio is observed [10,20].

A graphical representation of the G_0/M_{DMT} ratio for the soils studied here ($I_D > 1.2$) plotted as a function of K_D is given in Figure 16 on a log–log scale. In this figure, the best fitting equation for sands ($I_D > 1.8$) and silts ($0.6 < I_D < 1.8$) proposed by Marchetti et al. [10], the upper sedimentary/lower residual boundary ($I_D > 1.2$) proposed by Cruz et al. [37], the best fitting equation for collapsible loess soils proposed by Berisavljević et al. [42], and the best fitting equations for silts and fine/silty sands proposed by Mlynarek et al. [43] are also included. It can be observed from Figure 16 that G_0/M_{DMT} decreases with increasing K_D , which is common for all soils.

Figure 16 also shows that the dots representing the studied soils were plotted above the lines proposed by Marchetti et al. [10], Cruz et al. [37], Berisavljević et al. [42], and Mlynarek et al. [43], mainly for $K_D < 3$, and the trend line for studied soils has a higher slope than that of all the other soils.

Table 1. Parameters A and B for use in Eq. 5 for various soil types.

Soil type	G_0/M_{DMT}	A	B	R^2 Coefficient	Reference
Clay ($I_D < 0.6$)	1–20	26.177	−1.0066	0.61	Marchetti et al. [10]
Silt ($0.6 < I_D > 1.8$)	1–10	15.686	−0.921	0.81	
Sand ($I_D > 1.8$)	0.5–3	4.5613	−0.7967	0.65	
Sandy silts, sands ($I_D > 1.2$)	–	6.5	−0.691	–	Cruz et al. [37]
Loess ($I_D > 1.8$)	10–50	17.58	−0.577	0.644	Berisavljević et al. [42]
Silt ($0.6 < I_D > 1.8$)	1–23	22.608	−0.608	0.708	Mlynarek et al. [43]
Fine/silty sand	0.3–5	16.716	−1.184	0.658	Mlynarek et al. [43]
Silty sands ($0.6 < I_D < 1.8$)	0.6–65	49.587	−1.62	0.706	This study

**Figure 16.** G_0/M_{DMT} ratio vs. K_D for the studied soil sites (bilogarithmic scale).

5. Conclusions

The results presented in this paper indicate the following.

1. V_s and G_0 profiles determined by the CH and DH tests, SCPT, SSPT, and SDMT show good agreement at the UNESP and USP research sites. Consequently, all techniques can be used to determine the shear wave velocity and hence the maximum shear modulus for both sites.
2. The comparison between the measured and estimated G_0 showed G_{mea}/G_{est} ratios that are higher than 1.3 up to 10 m in depth for the UNESP research site, and 12 m in depth for the USP research site. It shows that the soil may have a microstructure (cementation/bonding and/or aging). It is related to the pedogenic and morphogenetic processes that occur in tropical soils.

3. The G_0/M_{DMT} vs. K_D and G_0/E_D vs. I_D charts indicate the presence of microstructure for both sites. The bonded structure of the tropical sandy soils studied produces G_0/E_D and G_0/M_{DMT} ratios that are systematically higher than those without a microstructure. If the soil has a significant microstructure, the classification charts and most of the existing empirical correlations may not always be applicable, and site- or geologic-specific modifications are required. In addition, almost all points for the investigated tropical soils show G_0/M_{DMT} ratios that are higher than those found in the literature, especially for $K_D < 3$. This clearly indicates that the soils investigated are highly structured, and thus the classical approaches for interpreting in situ tests may not always be applicable and site-specific modifications may be required.
4. It is possible to obtain a rough estimate of G_0 by using the DMT's intermediate parameters (I_D , K_D , and E_D) and by the constrained modulus (M_{DMT}) for the studied tropical soil sites, mainly during preliminary investigations when seismic measurements are not available. However, direct V_s measurements by seismic tests such as the SCPTu and the SDMT should be recommended.

Author contributions

Breno Padovezi Rocha: conceptualization, data curation, methodology, validation, writing – original draft, writing – review & editing. Luis Pedro Rojas Herrera: conceptualization, methodology, validation. Heraldo Luiz Giacheti: formal analysis, supervision, writing – review, funding acquisition, project administration, resources

Use of AI tools declaration

The authors declare they have not used artificial intelligence (AI) tools in the creation of this article.

Acknowledgments

The authors gratefully acknowledge the financial support from FAPESP (the São Paulo Research Foundation; Grant # 2015/17260-0) and CNPq (the National Council for Scientific and Technological Development; Grant # 2015/308895).

Conflict of interest

The authors have no conflicts of interest to declare. All co-authors have observed and affirmed the contents of the paper and there is no financial interest to report.

References

1. Schnaid F, Nierwinski HP, Odebrecht E (2020) Classification and State-Parameter Assessment of Granular Soils Using the Seismic Cone. *J Geotech Geoenvironmental Eng* 146. [https://doi.org/10.1061/\(ASCE\)GT.1943-5606.0002306](https://doi.org/10.1061/(ASCE)GT.1943-5606.0002306)

2. Rocha BP, Silveira IA, Rodrigues RA, et al. (2023) Identifying Collapsible Soils from Seismic Cone (SCPT): A Qualitative Approach. *Buildings* 13: 830. <https://doi.org/10.3390/buildings13030830>
3. Rocha BP, de Carvalho Rodrigues AL, Rodrigues RA, et al. (2022) Using a Seismic Dilatometer to Identify Collapsible Soils. *Int J Civ Eng* 20: 857–867. <https://doi.org/10.1007/s40999-021-00687-9>
4. Bang ES, Kim DS (2007) Evaluation of shear wave velocity profile using SPT based uphole method. *Soil Dyn Earthq Eng* 27: 741–758. <https://doi.org/10.1016/j.soildyn.2006.12.004>
5. Atkinson JH (2000) Non-linear soil stiffness in routine design. *Géotechnique* 50: 487–508. <https://doi.org/10.1680/geot.2000.50.5.487>
6. Dos Santos RA, Rocha BP, Giachetti HL (2020) DMT for Load-Settlement Curve Prediction in a Tropical Sandy Soil Compared to Plate Load Tests. *Geotech Test J* 43: 113–131. <https://doi.org/10.1520/GTJ20180079>
7. Wang Z, Zhang N, Cai G, et al. (2019) Field Investigation of Maximum Dynamic Shear Modulus of Clay Deposit Using Seismic Piezocone. *Int J Civ Eng* 17: 699–708. <https://doi.org/10.1007/s40999-018-0306-z>
8. Hunter J, Benjumea B, Harris J, et al. (2002) Surface and downhole shear wave seismic methods for thick soil site investigations. *Soil Dyn Earthq Eng* 22: 931–941. [https://doi.org/10.1016/S0267-7261\(02\)00117-3](https://doi.org/10.1016/S0267-7261(02)00117-3)
9. Stokoe KH, Joh SH, Woods RD (2004) Some contributions of in situ geophysical measurements to solving geotechnical engineering problems., *2nd International Conference on Site Characterization*, 97–132.
10. Marchetti S, Monaco P, Totani G, et al. (2008) In situ tests by seismic dilatometer (SDMT), In: Laier JE, Crapps DK, Hussein MH (Eds.), *From research to practice in geotechnical engineering, ASCE Geotech. Special Publication No. 180 (honoring Dr. John H. Schmertmann)*, 292–311.
11. Vargas M (1985) The Concept of Tropical Soils, In: Solos AB de M dos (Ed.), *1st International Conference on Geomechanics in Tropical Lateritic and Saprolitic Soils*, Brasilia, 101–134.
12. Fernandes J, Rocha B, Giachetti H (2023) Maximum shear modulus and modulus degradation curves of an unsaturated tropical soil. *Soils Rocks* 46: e2023013122. <https://doi.org/10.28927/SR.2023.013122>
13. ASTM D4428-07 (2007) Standard Test Methods for Crosshole Seismic Testing. *ASTM Int West Conshohocken, PA* 11.
14. ASTM D7400-19 (2019) Standard Test Methods for Downhole Seismic Testing, West Conshohocken, PA, ASTM International.
15. Campanella RG, Stewart WP (1992) Seismic cone analysis using digital signal processing for dynamic site characterization. *Can Geotech J* 29: 477–486. <https://doi.org/10.1139/t92-052>
16. Karl L, Haegeman W, Degrande G (2006) Determination of the material damping ratio and the shear wave velocity with the Seismic Cone Penetration Test. *Soil Dyn Earthq Eng* 26: 1111–1126. <https://doi.org/10.1016/j.soildyn.2006.03.001>
17. Pedrini RAA, Rocha BP, Giachetti HL (2018) The Up-Hole Seismic Test Together with the SPT: Description of the System and Method. *Soils Rocks* 41: 133–148. <https://doi.org/10.28927/SR.412133>
18. Marchetti S (1980) In Situ Tests by Flat Dilatometer. *J Geotech Eng Div* 106: 299–321. <https://doi.org/10.1061/AJGEB6.0000934>

19. Marchetti S, Monaco P (2018) Recent Improvements in the Use, Interpretation, and Applications of DMT and SDMT in Practice. *Geotech Test J* 41: 837–850. <https://doi.org/10.1520/GTJ20170386>
20. Monaco P, Marchetti S, Totani G, et al. (2009) Interrelationship between small strain modulus G_0 and operative modulus, In: Kokusho T, Tsukamoto Y, Yoshimine M (Eds.), *Performance-based Design in Earthquake Geotechnical Engineering- from case history to practice, proc. IS-Tokyo 2009*, Tsukuba, 1315–1323.
21. Robertson PK (2016) Cone penetration test (CPT)-based soil behaviour type (SBT) classification system — an update. *Can Geotech J* 53: 1910–1927. <https://doi.org/10.1139/cgj-2016-0044>
22. Cotecchia F, Chandler RJ (1997) The influence of structure on the pre-failure behaviour of a natural clay. *Géotechnique* 47: 523–544. <https://doi.org/10.1680/geot.1997.47.3.523>
23. Cuccovillo T, Coop MR (1997) Yielding and pre-failure deformation of structured sands. *Géotechnique* 47: 491–508. <https://doi.org/10.1680/geot.1997.47.3.491>
24. Yamamuro JA, Wood FM, Lade PV (2008) Effect of depositional method on the microstructure of silty sand. *Can Geotech J* 45: 1538–1555. <https://doi.org/10.1139/T08-080>
25. Leroueil S, Vaughan PR (1990) The general and congruent effects of structure in natural soils and weak rocks. *Géotechnique* 40: 467–488. <https://doi.org/10.1680/geot.1990.40.3.467>
26. Lambe TW, Whitman R V. (1969) Soil Mechanics, New York, John Wiley & Sons.
27. Berisavljević D, Berisavljević Z (2019) Determination of the presence of microstructure in a soil using a seismic dilatometer. *Bull Eng Geol Environ* 78: 1709–1725. <https://doi.org/10.1007/s10064-018-1234-5>
28. Giacheti HL, Bezerra RC, Rocha BP, et al. (2019) Seasonal influence on cone penetration test: An unsaturated soil site example. *J Rock Mech Geotech Eng* 11: 361–368. <https://doi.org/10.1016/j.jrmge.2018.10.005>
29. De Mio G (2005) Geological conditioning aspects for piezocone test interpretation for stratigraphical logging in geotechnical and geo-environmental site investigation (in Portuguese).
30. Nogami JS, Villibor DF (1981) Uma nova classificação de solos para finalidades rodoviárias, *Simpósio Brasileiro de Solos Tropicais em Engenharia*, Rio de Janeiro, ABMS, 30–41.
31. Rocha BP, Giacheti HL (2018) Site Characterization of a Tropical Soil by In Situ Tests. *DYNA* 85: 211–219. <https://doi.org/10.15446/dyna.v85n206.67891>
32. Rocha BP, Rodrigues RA, Giacheti HL (2021) The Flat Dilatometer Test in an Unsaturated Tropical Soil Site. *Geotech Geol Eng* 39: 5957–5969. <https://doi.org/10.1007/s10706-021-01849-1>
33. Vitali OPM, Pedrini RAA, Oliveira LPR, et al. (2012) Developing a System for Down-Hole Seismic Testing Together with the CPTU. *Soils Rocks* 35: 75–87. <https://doi.org/10.28927/SR.351075>
34. NBR 9604 AN (2024) Soil — Opening of a well or inspection trench, with removal of disturbed and undisturbed samples — Procedure, Rio de Janeiro.
35. Cho GC, Santamarina JC (2001) Unsaturated Particulate Materials—Particle-Level Studies. *J Geotech Geoenvironmental Eng* 127: 84–96. [https://doi.org/10.1061/\(ASCE\)1090-0241\(2001\)127:1\(84\)](https://doi.org/10.1061/(ASCE)1090-0241(2001)127:1(84))
36. Gutierrez NHM, de Nóbrega MT, Vilar OM (2009) Influence of the microstructure in the collapse of a residual clayey tropical soil. *Bull Eng Geol Environ* 68: 107–116. <https://doi.org/10.1007/s10064-008-0180-z>

37. Cruz N, Rodrigues C, Viana Da Fonseca A (2012) Detecting the presence of cementation structures in soils, based in DMT interpreted charts, In: Coutinho RQ, Mayne PW (Eds.), *4th International Conference on Site Characterization (ISC4)*., Porto de Galinhas, Taylor & Francis Group, 1723–1728.
38. Tanaka H, Tanaka M (1998) Characterization of Sandy Soils Using CPT and DMT. *Soils Found* 38: 55–65. https://doi.org/10.3208/sandf.38.3_55
39. Hryciw RD (1990) Small-Strain-Shear Modulus of Soil by Dilatometer. *J Geotech Eng* 116: 1700–1716. [https://doi.org/10.1061/\(ASCE\)0733-9410\(1990\)116:11\(1700\)](https://doi.org/10.1061/(ASCE)0733-9410(1990)116:11(1700))
40. Leonards GA, Frost JD (1988) Settlement of Shallow Foundations on Granular Soils. *J Geotech Eng* 114: 791–809. [https://doi.org/10.1061/\(ASCE\)0733-9410\(1988\)114:7\(791\)](https://doi.org/10.1061/(ASCE)0733-9410(1988)114:7(791))
41. Baldi G, Bellotti R, Ghionna V, et al. (1989) Modulus of Sands from CPT's and DMT's, *XII ICSMFE*, Rio de Janeiro, 165–170.
42. Berisavljević D, Berisavljević Z, Čebašek V, et al. (2014) Characterisation of collapsing loess by seismic dilatometer. *Eng Geol* 181: 180–189. <https://doi.org/10.1016/j.enggeo.2014.07.011>
43. Mlynarek Z, Wierzbicki J, Monaco P (2022) Use of DMT and CPTU to assess the G0 profile in the subsoil, In: Tonni G& (Ed.), *Cone Penetration Testing 2022*, Taylor & Francis Group, 7. <https://doi.org/10.1201/9781003308829-82>



AIMS Press

© 2025 the Author(s), licensee AIMS Press. This is an open access article distributed under the terms of the Creative Commons Attribution License (<https://creativecommons.org/licenses/by/4.0/>)